ELSEVIER

Ceramics International 26 (2000) 447–453

CERAMICS INTERNATIONAL

Sintering and physicochemical properties of compositions in the $SiC–Al_2O_3–La_2O_3–Cr_2O_3$ system II. Oxidation resistance of pressureless sintered compacts in the $SiC–Al_2O_3–La_2O_3–Cr_2O_3$ system

Andrei Kirianov[a,b,*], Akira Yamaguchi[a]

[a]*Department of Materials Science and Engineering, Nagoya Institute of Technology, Gokiso-cho, Showa-ku, Nagoya 466-8555, Japan*
[b]*Department of Chemical Technology of Ceramics, Mendeleyev University of Chemical Technology of Russia, Miusskaya sq. 9, Moscow 125190, Russia*

Received 15 May 1999; received in revised form 20 May 1999; accepted 1 July 1999

Abstract

Compacts prepared from SiC (70–55 wt%), Al_2O_3 (10 wt%) and $LaCrO_3$ (20–35 wt%) by pressureless sintering in carbon at 1700°C were studied for their oxidation resistance in air at 1300, 1400 and 1500°C. The oxidation resistance of the material at 1500°C was dependent on the quantity of $La_2O_3–Al_2O_3–SiO_2$ melt, which diffused from inside to the surface of the compacts. Instead, chromium compounds were retained in the material and barred the melt diffusion. Nevertheless, at 1300°C, La_2O_3 of the compacts reacted with SiO_2 and gave a dependable protective layer of lanthanum silicates.

Keywords: B. Electron microscopy; D. SiC; D. Al_2O_3; D. Silicate; Oxidation resistance

1. Introduction

Silicon carbide is widely studied due to its promising application and remarkable properties such as high bending strength and oxidation resistance. However, due to a strong covalent bonding in SiC, the techniques, which allows us to obtain well-sintered SiC ceramic materials, use hot, or hot isostatic pressing or temperatures higher than 2000°C and use of sintering additives such as alumina or alumina with yttria or other rare-earth oxides [1–3]. In part I of the present study, it was shown that compositions in the $SiC–Al_2O_3–La_2O_3–Cr_2O_3$ system could be considered as alternative material to the pure SiC material. Ceramic bodies of these compositions containing up to 60 wt% SiC sinter up to 90% of theoretical density already at a temperature as low as 1700°C and have fracture toughness of about 5 MPa $m^{1/2}$ as a result of in-situ synthesized $LaAlO_3$ and chromium carbides. However, possible interaction between SiC and $LaAlO_3$ or chromium compounds under oxidation atmosphere requires investigation of the stability of the material and examination of its oxidation resistance at high temperature.

It is known that the oxidation resistance of SiC materials containing oxide components such as alumina is strongly dependent on the contents of the oxide, as was reported by Singhal [4,5]. The oxide is suggested to promote the formation of a liquid phase along with other impurities, which are usually present in small quantities. The oxidation tests of SiC containing up to 12 wt% Al_2O_3 in pure dry oxygen at 1370°C showed a parabolic oxidation behavior. Weight gains of compacts were observed to grow with an increase in Al_2O_3 which, along with impurities, was considered to originate the formation of a low melting phase.

On the other hand, Matsumura et al. [6] observed a favorable effect of chromium oxide additions on the oxidation resistance of $Al_2O_3–SiC–C$ ceramics in air at 1400°C. This effect is considered to be caused by the formation of a protective silica layer, which was promoted by reaction between SiC and Cr_2O_3.

Thus, this paper considers the roles of all included oxide components — La_2O_3, chromium compounds and

* Corresponding author: Tel.: +81-052-735-5293; fax: +81-052-735-5294.
E-mail address: ankir@mse.nitech.ac.jp (A. Kirianov).

0272-8842/00/$20.00
PII: S0272-8842(99)00079-6

Al_2O_3 in an oxidation behavior of the compositions in $SiC–Al_2O_3–La_2O_3–Cr_2O_3$ system at 10 wt% Al_2O_3, the ceramic bodies of which showed the best densification.

We also report an attempt to elucidate the processes which proceeded during oxidation and gave rise to the formation of an oxidized layer.

2. Experimental

2.1. Materials

Ultrafine β-SiC (Betarundum by Ibiden Co., Ltd) with mean particle size of 0.28 μm and containing about 0.8 wt% free carbon and about 0.43 wt% free silica was used. Al_2O_3 (Taimicron by Taimei Chemicals Co., Ltd) of 99.99% purity grade with mean particle size of 0.1 μm was used. $LaCrO_3$ synthesized from reagent grade Cr_2O_3 and La_2O_3 (Kishida Chemicals Co., Ltd) of 99.9 and 99.99% purity grades, respectively, were used.

As synthesized $LaCrO_3$ had an average grain size of 2 μm, it was determined by SEM observation.

2.2. Fabrication of ceramics

The $LaCrO_3$, Al_2O_3 and SiC of compositions shown in Table 1 were first thoroughly mixed in ethanol, dried and again mixed with an aqueous solution containing 2–3 wt% of polyethylene glycol. The resultant mixtures were dried, passed through a 250 μm sieve, prepressed at 10 MPa and cold isostatically pressed at 100 MPa to form compacts of 20×20×14–16 mm. The compacts were buried with graphite powder enclosed in an alumina crucible fitted with a tight alumina lid and heated at 1700°C for 2 h.

2.3. Measurements

The compacts were characterized for their density and open porosity with the Archimedes' method. Phase compositions of compacts after sintering were determined by X-ray diffraction analysis (XRD).

The oxidation behaviors of the compacts were studied by continuous thermogravimetry using automatic electrobalance. Polished samples of 10 × 18 mm, 2.5–3 mm thick, were placed on platinum gauze and suspended from the balance with a platinum wire in such a way as to be held in a hot zone of a resistance pipe furnace. Oxidation tests were performed at 1300, 1400 and 1500°C in static air.

The oxidized layer structures of samples tested at 1500°C were observed by SEM using the thin cross-sections which were fine polished with 0.5 μm diamond and etched in a 2% HF water solution for about 1–1.5 min. The element distribution over the oxidized layer and inside of the compact was done with X-ray diffraction element analyzer (EDAX). After oxidation, the surfaces of the oxidized layers and body of the compacts with removed oxidized layer were also examined with the aid of X-ray diffraction analysis (XRD).

The interface between the oxidized layer and compact was analyzed by laser Raman spectroscopy.

Table 1
The physicochemical properties of the compacts sintered in graphite at 1700°C for 2 h

Starting composition (wt%)			Relative density (%)	Open porosity (%)
SiC	$LaCrO_3$	Al_2O_3		
70	20	10	84.9	4.9
65	25	10	85.4	4
60	30	10	86.7	3.2
55	35	10	87.8	2.8

3. Results and discussion

The sintered compacts before oxidation tests contained SiC and $LaAlO_3$ phases as they were determined by XRD analysis. The compacts were sintered to about 85–88% of theoretical density and had low open porosity of 3–5% as shown in Table 1. The microstructure of a compact sintered with 30 wt% $LaCrO_3$ is shown in Fig. 1. According to optical microscopic observation,

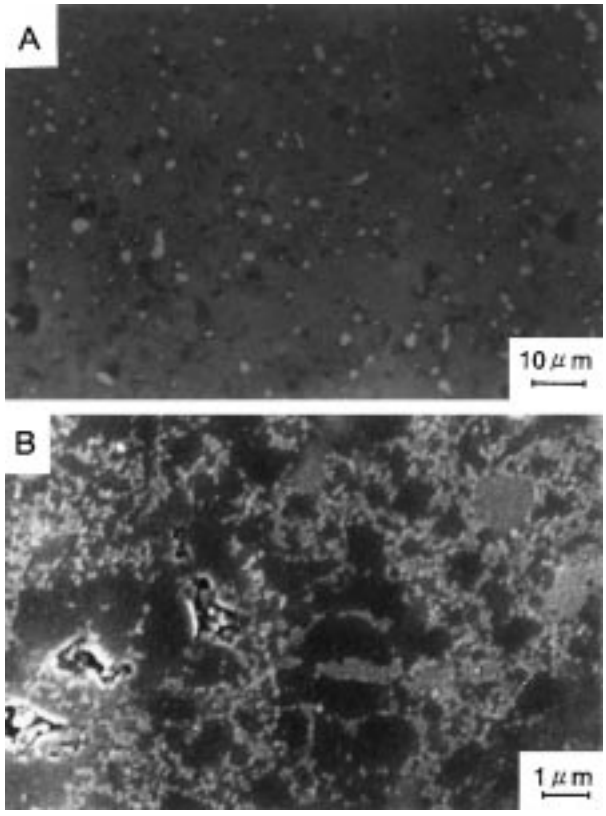

Fig. 1. Optical photograph (A) and SEM micrograph (B) of microstructure of $60SiC–30LaCrO_3–10Al_2O_3$ compact as sintered at 1700°C for 2 h in graphite.

the compact had a structure of matrix with 2–4 μm whitish inclusions (see Fig. 1A). These inclusions are determined by element analysis (see Table 2) to be some kind of chromium carbides, which were formed by a reaction of chromium oxide of the starting $LaCrO_3$ and SiC. SEM observation showed that the matrix is comprised of dark silicon carbide grains with fine crystals found over the grain boundaries of silicon carbide grains (see Fig. 1B). Regarding the data of the compact XRD analysis, these fine grains are likely to be $LaAlO_3$ crystallized out from the liquid phase.

The results of oxidation tests at 1300, 1400 and 1500°C, presented as weight gain-vs-time curves of compacts with 25 to 35 wt% of starting $LaCrO_3$, are shown in Fig. 2. As seen for all test temperatures, the weight gain is characterized by faster growth over the first hours of oxidation, slowing down with longer duration of oxidation test. The latter effect is clearly seen on the curves of materials during tests at 1300 and 1400°C.

In particular, the compact with 20 wt% $LaCrO_3$ showed almost a stop of the weight gain after 10 h at 1300°C (see Fig. 2). Such behavior is believed to be related to the effect of a protective layer which is formed. As shown in Figs. 3b and 4a, XRD analysis of oxidized surfaces revealed the peaks of the crystobalite phase and some unidentified peaks, which probably appeared as superposing of differently oriented inclusions in the oxidized layer. However, at 1300°C, the oxidized surface of the compact with 20 wt% $LaCrO_3$ showed the strong peaks of phases different from crystobalite and identified with the aid of X-ray element analysis as lanthanum silicate. Its needlelike crystals formed the oxidized layer of the compact at 1300°C (see Fig. 5 and Table 2). At 1500°C, the oxidized layers of materials differed by a structure in relation to the starting $LaCrO_3$ content, as shown in Fig. 6 and Table 2. Up to 25 wt% $LaCrO_3$, the oxidized layer is made up of a glassy phase (gray area marked as *g*) and crystals of crystobalite (dark grains marked as *c*). With higher content of starting $LaCrO_3$, it is comprised

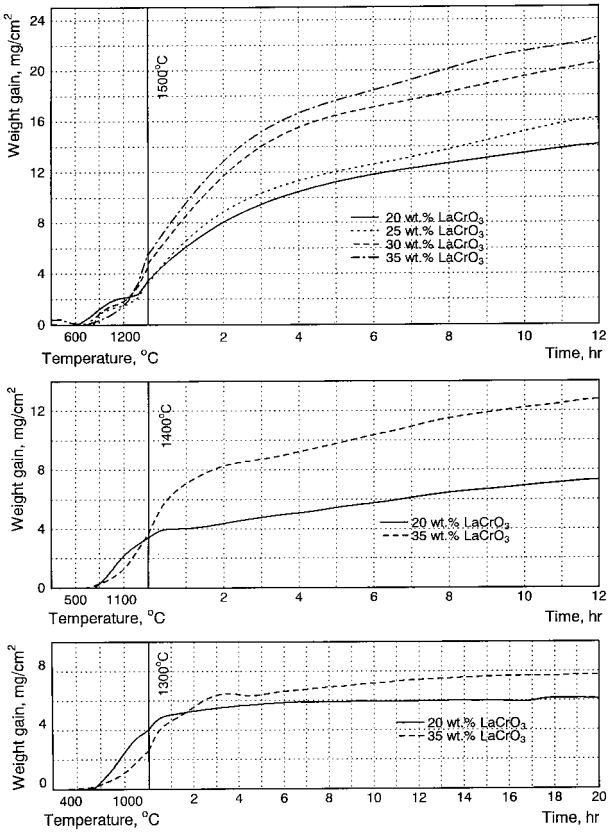

Fig. 2. Oxidation resistance of SiC–$LaCrO_3$–Al_2O_3 compacts in static air at 1300, 1400 and 1500°C.

of needlelike crystals of lanthanum silicate (marked as *s*) and the glass phase. Rounded pores seen in the oxidized layers are entrapped gases of SiO and CO. As follows from Fig. 7 showing element distribution over one of the compacts, the oxidized layer is separated form the rest of the compact with an interface layer where La, Al, Cr and Si are not present while carbon was identified with the use of Raman spectroscopy by a characteristic shift peak at 1570 cm^{-1} (see Fig. 8) [8]. The carbon is believed to be

Table 2
The results of element analysis for the oxydized layers and the inside parts of the compacts

Starting composition (wt%)			Element (at%)					
SiC	$LaCrO_3$	Al_2O_3	O	Al	Si	La	Cr	Remarks
70	20	10	54.8	0	43.1	2.3	0	SiO_2, dark grain in the oxidized layer, *c*
			–	10.7	50	36.8	3.12	Lanthanum silicates, needlelike grains found in the oxidized layer after 20 h at 1300°C in air
65	25	10	54.6	0.7	41.9	2.5	0.23	SiO_2, dark grain in the oxidized layer, *c*
60	30	10	54.3	0	42.8	2.87	0	SiO_2, dark grain in the oxidation layer, *c*
			38.1	2.2	20.3	39.2	0.2	Lanthanum silicates, needlelike grain in the oxidized layer, *s*
			45.8	7.3	24.9	21.1	0.9	Grey area of lanthanum–alumina–silica glass, *g*
			10.9	4.4	74.5	5.8	4.4	SiC and $LaAlO_3$, the inside part of the compact
			7.9	2.2	28.6	4	57.2	Chromium carbide, white inclusions in the inside part of the compact
55	35	10	56.8	0.47	41.1	1.37	0.23	SiO_2, dark grain in the oxidized layer, *c*
			43.3	2.5	21.7	31.9	0.5	Lanthanum silicates, needlelike grain in the oxidized layer, *s*
			45.1	6.9	25.1	22.7	0.3	Grey area of lanthanum–alumina–silica glass, *g*

originated by oxidation of SiC under low partial pressure of oxygen with evolution of SiO gas as follows [9]:

$$2SiC + O_2 \rightarrow C + 2SiO.$$

X-ray element analysis of the glass phase of the oxidized layer showed that it included silica, aluminum and lanthanum oxides (see Table 2). Data of element analysis showed that the concentration of La in the oxidized layer is 4–5 times higher than that in the inside of the compact (see Table 2). $LaAlO_3$ or lanthanum-containing phase was also not identified by XRD analysis for the inside part, as seen in Fig. 3c. Therefore, $LaAlO_3$ crystals found over the grain boundaries of SiC were

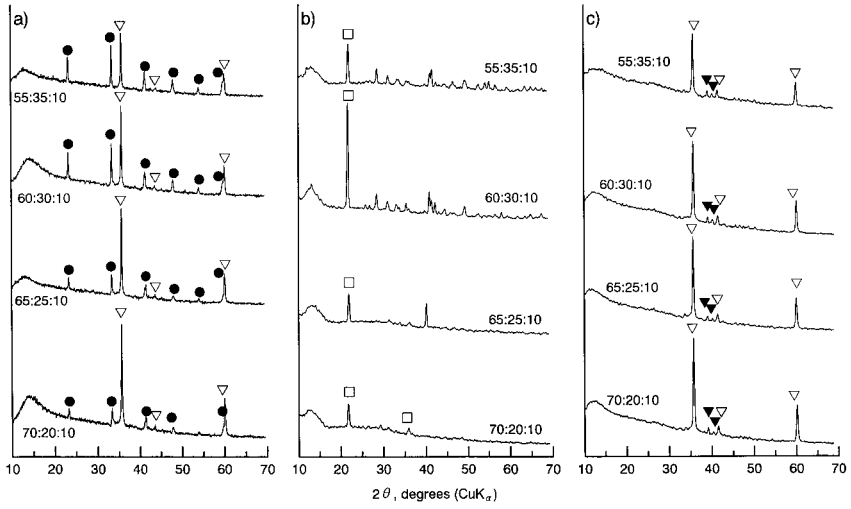

Fig. 3. XRD patterns of the compacts as sintered at 1700°C (a), oxidized surfaces of the compacts (b) and inside parts after oxidation in air at 1500°C (c): (▽) SiC, (□) crystobalite, (●) $LaAlO_3$, (▼) Cr_3C_2, unmarked peaks are unidentified phase.

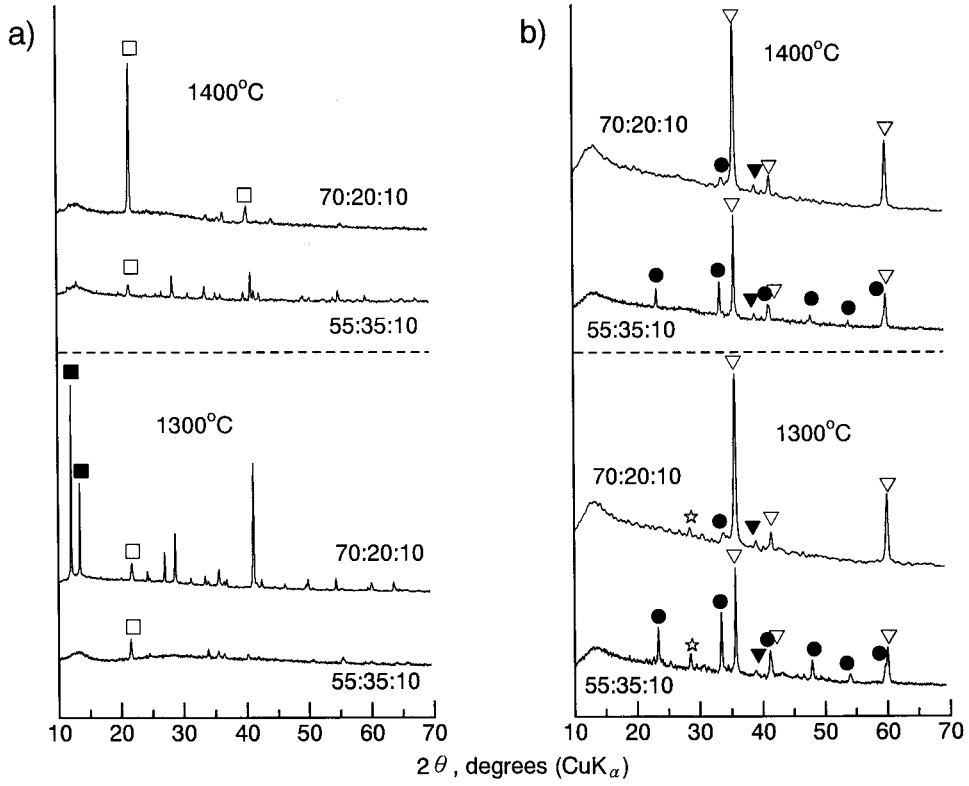

Fig. 4. XRD patterns of the oxidized surfaces of materials (a) and the inside part (b) after oxidation test at 1300 and 1400°C: (▽) SiC, (□) SiO_2 crystobalite, (●) $LaAlO_3$, (■) $La_2Si_2O_7$, (▼) Cr_3C_2, (bfl) chromium oxide (CrO_2), unmarked peaks are unidentified phase.

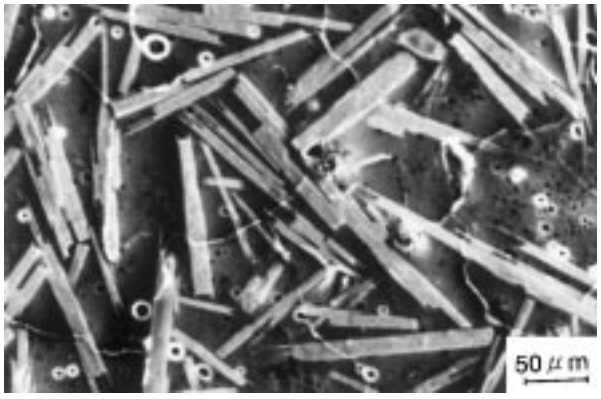

Fig. 5. SEM micrograph of the oxidized layer of 70SiC–20$LaCrO_3$–10Al_2O_3 compact after 20 h in air at 1300°C.

reacted with silica and diffused as a melt to the oxidation surface. According to Shiokawa et al. [7], a melt in the La_2O_3–Al_2O_3–SiO_2 system can exist, beginning from 1400°C at a silica content as low as 20 wt%. Data of element analysis also showed that La_2O_3 was, in particular, diffused better than Al_2O_3, since the concentrations of Al did not differ greatly between the oxidized layer and the inside part. Cr, as seen from Fig. 7, was found both in the oxidized layer and inside part but in different patterns. The Cr distribution in the inside part resembles the pattern of chromium carbide inclusions before oxidation, suggesting it to be unoxidized chromium carbide, as shown by XRD data in Fig. 3c. In the oxidized layer, Cr as chromium oxide was found close to the interface layer in the form of streaks arranged

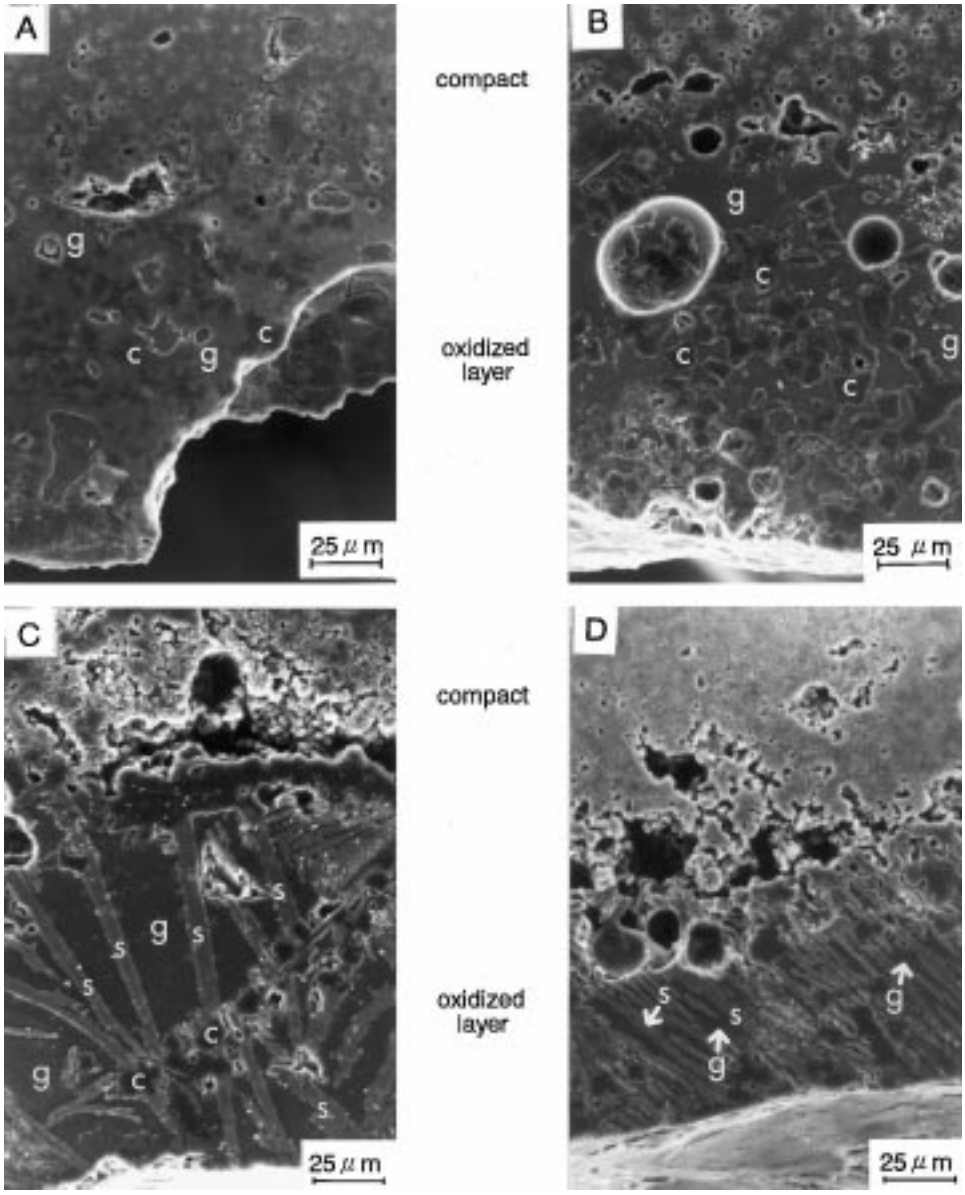

Fig. 6. SEM micrographs of oxidized layers of compacts oxidized in air at 1500°C for 12 h: (A) 70 wt% SiC, 10 wt% Al_2O_3, 20 wt% $LaCrO_3$; (B) 65 wt% SiC, 10 wt% Al_2O_3, 25 wt% $LaCrO_3$; (C) 60 wt% SiC, 10 wt% Al_2O_3, 30 wt% $LaCrO_3$; (D) 55 wt% SiC, 10 wt% Al_2O_3, 35 wt% $LaCrO_3$].

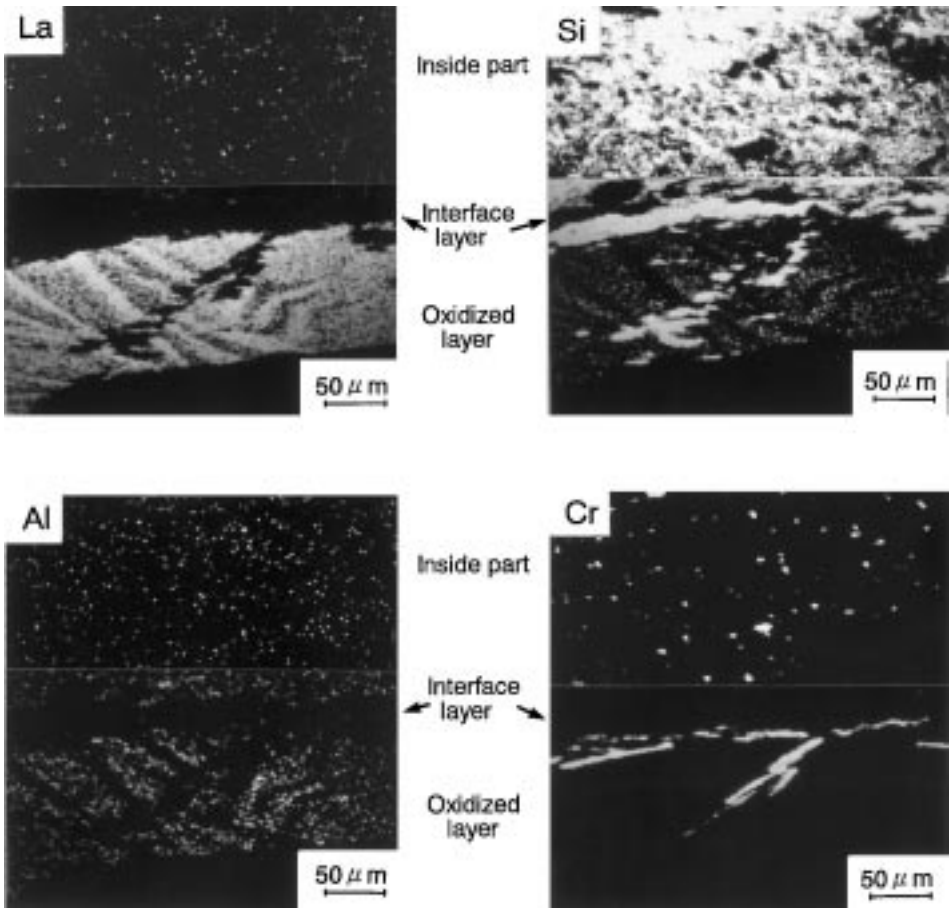

Fig. 7. The graphs of element distribution over the oxidized compact of $60SiC–30LaCrO_3–10Al_2O_3$ composition after 12 h at 1500°C in air.

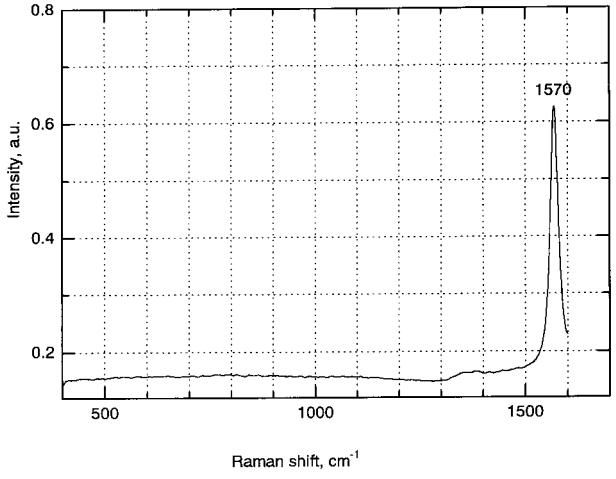

Fig. 8. The results of Raman spectroscopy analysis for the interface layer of the oxidized 60:30:10 composition compact.

along the oxidation surface. Since the concentration of Cr in the glass phase is negligible (Table 2), chromium compounds would rather not be transported with the liquid phase from the inside part of the material. It is suggested that, on oxidation, the La_2O_3-rich melt, which was gradually moving out towards a surface of the compact, drove the chromium compounds out to a periphery of the oxidized layer and arranged them in a streak-like way.

The above observation suggests that the oxidation resistance of the material should be mostly affected by amounts of the La-rich liquid phase formed. Thus, Fig. 2 shows that the higher content of La_2O_3 (from the starting $LaCrO_3$) in the material resulted in higher weight gains and worse oxidation resistance. On the other hand, chromium compounds, since they were retained by the compact, are not likely to affect adversely the oxidation resistance of the material. However, at 1300°C, when the temperature was considered to be low enough to cause the formation of the liquid phase in large amounts, La_2O_3 promoted the formation of a dependable protective layer from the lanthanum silicate crystals at 20 wt% $LaCrO_3$. XRD analysis, as shown in Fig. 4b, also proved a smaller diffusion of La_2O_3 from the compact where $LaAlO_3$ phase was still present at 1300°C compared with the results at 1500°C.

4. Conclusions

The oxidation of the compositions in $SiC–La_2O_3–Cr_2O_3–Al_2O_3$ system at 10 wt% Al_2O_3 was studied in air

at 1300, 1400 and 1500°C. The increase in La_2O_3 content via $LaCrO_3$ addition gave the increase in the weight gain of material on oxidation. La_2O_3 in the presence of Al_2O_3 is responsible for the quantity of La_2O_3–Al_2O_3–SiO_2 liquid phase formed on oxidation. This liquid phase transports La_2O_3 from the inside part of the compact to the surface that impairs the oxidation resistance of materials at temperatures higher than 1400°C. The chromium compounds due to bad solubility in La_2O_3–Al_2O_3–SiO_2 liquid phase were retained by the compacts and did not have an adverse effect on the oxidation resistance of the material.

At lower than 1400°C, La_2O_3, along with silica, provided the protective layer from the lanthanum silicates.

Acknowledgement

The authors thank Associate Professor D. Nishikawa for his help and useful advice in carrying out X-ray diffraction element analysis.

References

[1] M.A. Mulla, V.D. Krstic, Pressureless sintering of β-SiC with Al_2O_3 additions, J. Mater. Sci. 29 (1994) 934–938.
[2] M. Omori, A.S. Akuma, T. Hirai, SiC sintered composite with Y_2O_3 and Al_2O_3, in: Ceramics Today — Tomorrow's Ceramics, Elsevier Science Publishers B. V., 1991, pp. 1327–1335.
[3] N.P. Padture, In situ-toughened silicon carbide, J. Am. Ceram. Soc. 77 (1994) 519–523.
[4] S.C. Singhal, Oxidation kinetics of hot-pressed silicon carbide in dry and wet oxygen, Am. Ceram. Soc. Bull. 53 (1974) 396.
[5] S.C. Singhal, F.F. Lange, Effect of alumina content on the oxidation of hot-pressed silicon carbide, J. Am. Ceram. Soc. 58 (1975) 433–435.
[6] T. Matsumura, T. Kitai, T. Hokii, The effect of chromia on the protection of alumina–SiC–C bricks against oxidation, Ceram. Trans. 4 (Adv. Refract. Technol.) (1989) 506–522.
[7] J. Shiokawa, G. Adachi, M. Tanaka, Phase relations in the system La_2O_3–Al_2O_3–SiO_2 at 1550°C, Asahi garasu kougyou gijutsu shyoureikai kenkyuhoukoku 14 (1968) 227–233.
[8] C.L. Renschler, A.P. Sylwester, L.V. Salgato, Carbon films from polyacrylonitrile, J. Mater. Res. 4 (1989) 452–457.
[9] JANAF, Thermochemical Data, 2nd ed., USA Nat. Bu. Stan., 1971.